Supplemental Material to: "Exponentially Improved Dispersive Qubit Readout with Squeezed Light"

Wei Qin[1,2,6,*] Adam Miranowicz[2,3], and Franco Nori[2,4,5]

[1] *Center for Joint Quantum Studies and Department of Physics, School of Science, Tianjin University, Tianjin 300350, China*
[2] *Theoretical Quantum Physics Laboratory, Cluster for Pioneering Research, RIKEN, Wako-shi, Saitama 351-0198, Japan*
[3] *Institute of Spintronics and Quantum Information, Faculty of Physics, Adam Mickiewicz University, 61-614 Poznań, Poland*
[4] *Center for Quantum Computing, RIKEN, Wako-shi, Saitama 351-0198, Japan*
[5] *Department of Physics, The University of Michigan, Ann Arbor, Michigan 48109-1040, USA*
[6] *Tianjin Key Laboratory of Low Dimensional Materials Physics and Preparing Technology, Tianjin University, Tianjin 300350, China*

Introduction

In this Supplemental Material, we investigate in detail dispersive qubit readout (DQR) with injected external squeezing (IES) in Sec. S1, and then the case with intracavity squeezing (ICS) in Sec. S2. We demonstrate that these two cases *cannot enable a significant and practically useful increase* in the signal-to-noise ratio (SNR). In Sec. S3, we show a detailed analysis of the qubit-cavity dispersive coupling enhanced by squeezing. In Sec. S4, we present more details of the derivation of the SNR of DQR with both IES and ICS. In this case, we find that, in sharp contrast to the case of using IES or ICS alone, their simultaneous use can lead to *an exponential improvement* of the SNR. In particular, for a short time measurement, the SNR is improved *exponentially with twice the squeezing parameter*. Finally, the effects of parameter mismatches in realistic experiments on our readout proposal are discussed in Sec. S5.

S1. Dispersive qubit readout with injected external squeezing

In this section, we discuss dispersive qubit readout (DQR) with injected external squeezing (IES). Specifically, we derive in detail the measurement signal, the measurement noise, and as a result, the signal-to-noise ratio (SNR). We demonstrate that IES is able to exponentially improve the SNR only in the two impractical limits $\kappa\tau \to 0$ and ∞, corresponding to a strong measurement tone and a long measurement time, respectively. However, in the regime $\kappa\tau \sim 1$, which is of most interest in experiments, a qubit-state-dependent rotation of squeezing becomes dominant and increases the overlap of the pointer states, thus largely limiting the SNR improvement. *Thus, IES cannot significantly improve the SNR at an experimentally feasible measurement time.*

We begin with the readout Hamiltonian given by

$$\hat{H} = \chi \hat{a}^\dagger \hat{a} \hat{\sigma}_z, \tag{S1}$$

where $\chi = g^2/\Delta$, with g denoting the coupling of the qubit to the cavity and Δ denoting their detuning. Moreover, $\hat{\sigma}_z$ is a Pauli operator of the qubit. Correspondingly, the Langevin equation of motion for the cavity mode $\hat{a}$ reads

$$\dot{\hat{a}} = -(\sigma\chi - i\kappa/2)\hat{a} - \sqrt{\kappa}\,\hat{a}_{\rm in}(t), \tag{S2}$$

where κ is the photon loss rate of the cavity. Here, the qubit has been assumed to be in a definite state, such that the operator $\hat{\sigma}_z$ has been rewritten as a c-number $\sigma = \pm 1$, corresponding to the excited and ground states of the qubit, respectively. Moreover, $\hat{a}_{\rm in}(t)$ represents the input field of the cavity. We assume that a squeezed vacuum reservoir, acting as IES, is injected into the cavity. In this case, the correlations for the noise operator $\hat{\mathcal{A}}_{\rm in}(t) = \hat{a}_{\rm in}(t) - \langle \hat{a}_{\rm in}(t)\rangle$ are:

$$\langle \hat{\mathcal{A}}^\dagger_{\rm in}(t)\,\hat{\mathcal{A}}_{\rm in}(t')\rangle = \sinh^2(r)\delta(t-t'), \quad \langle \hat{\mathcal{A}}_{\rm in}(t)\,\hat{\mathcal{A}}^\dagger_{\rm in}(t')\rangle = \cosh^2(r)\delta(t-t'), \tag{S3}$$

$$\langle \hat{\mathcal{A}}_{\rm in}(t)\,\hat{\mathcal{A}}_{\rm in}(t')\rangle = \frac{1}{2}e^{i\varphi}\sinh(2r)\delta(t-t'), \quad \langle \hat{\mathcal{A}}^\dagger_{\rm in}(t)\,\hat{\mathcal{A}}^\dagger_{\rm in}(t')\rangle = \frac{1}{2}e^{-i\varphi}\sinh(2r)\delta(t-t'), \tag{S4}$$

* qin.wei@tju.edu.cn

where r is the squeezing parameter of IES and φ is the reference phase. It follows, after formally integrating Eq. (S2), that

$$\hat{a}(t) = \exp[-i(\sigma\chi - i\kappa/2)t]\hat{a}(0) - \sqrt{\kappa}\int_0^t \exp[-i(\sigma\chi - i\kappa/2)(t-s)]\hat{a}_{\rm in}(s)ds, \tag{S5}$$

where the initial measurement time has been assumed to be zero for simplicity.

The dispersive coupling of the cavity mode and the qubit causes the qubit state information to be encoded in the output quadrature,

$$\hat{\mathcal{Z}}_{\rm out}(t) = \hat{a}_{\rm out}(t)\exp(-i\phi_h) + \hat{a}^\dagger_{\rm out}(t)\exp(i\phi_h), \tag{S6}$$

which can be recorded by homodyne detection. Here, ϕ_h is the measurement angle and $\hat{a}_{\rm out}(t) = \hat{a}_{\rm in}(t) + \sqrt{\kappa}\hat{a}(t)$ refers to the output field of the cavity. The essential parameter quantifying homodyne detection is the SNR. To evaluate the SNR, we typically use the measurement operator,

$$\hat{M} = \sqrt{\kappa}\int_0^\tau dt\,\hat{\mathcal{Z}}_{\rm out}(t), \tag{S7}$$

with τ being the measurement time. Its average $\langle\hat{M}\rangle$ corresponds to the qubit-state-dependent signal. The fluctuation noise of the measurement operator $\hat{M}$ is described by $\hat{M}_N = \hat{M} - \langle\hat{M}\rangle$. With these quantities, the SNR is defined as

$$\mathrm{SNR} = \frac{\left|\langle\hat{M}\rangle_\uparrow - \langle\hat{M}\rangle_\downarrow\right|}{\sqrt{\langle\hat{M}_N^2\rangle_\uparrow + \langle\hat{M}_N^2\rangle_\downarrow}}, \tag{S8}$$

where the arrows $\uparrow$ (i.e., $\sigma = +1$) and $\downarrow$ (i.e., $\sigma = -1$) refer to the excited and ground states of the qubit, respectively.

Consider a coherent measurement tone $\langle\hat{a}_{\rm in}(t)\rangle = \alpha_{\rm in}e^{i\phi_{\rm in}}$. The averaged cavity field can be expressed as

$$\langle a(t)\rangle = i\frac{\sqrt{\kappa}\alpha_{\rm in}e^{i\phi_{\rm in}}}{\sigma\chi - i\kappa/2}\left\{1 - \exp[-i(\sigma\chi - i\kappa/2)t]\right\}, \tag{S9}$$

under the initial condition $\langle\hat{a}(0)\rangle = 0$, and the number of cavity photons is accordingly given by

$$n(t) = \langle\hat{a}^\dagger(t)\,\hat{a}(t)\rangle = \sinh^2(r) + \frac{4\alpha_{\rm in}^2}{\kappa}\cos^2(\psi)\left[1 + e^{-\kappa t} - 2\cos(\chi t)e^{-\kappa t/2}\right], \tag{S10}$$

where $\tan(\psi) = 2\chi/\kappa$. Here, we have assumed that at the initial measurement time $t = 0$, the cavity subject to IES is already in a steady state. Then, we find

$$\langle M\rangle_\uparrow - \langle M\rangle_\downarrow = \frac{4\alpha_{\rm in}}{\sqrt{\kappa}}\sin(2\psi)\sin(\phi_h - \phi_{\rm in})\left\{\kappa\tau - 4\cos^2(\psi)\left[1 - \frac{\sin(2\psi + \chi\tau)}{\sin(2\psi)}e^{-\kappa t/2}\right]\right\}. \tag{S11}$$

Note that this expression of the signal separation is the same as that in the standard dispersive readout of no squeezing.

We now derive the measurement noise. The quantum fluctuation operator, $\hat{\mathcal{A}}_{\rm out}(t) = \hat{a}_{\rm out}(t) - \langle\hat{a}_{\rm out}(t)\rangle$, of the output field has the form

$$\hat{\mathcal{A}}_{\rm out}(t) = \hat{\mathcal{A}}_{\rm in}(t) + \sqrt{\kappa}\hat{\mathcal{A}}(t). \tag{S12}$$

Here, $\hat{\mathcal{A}}(t) = \hat{a}(t) - \langle\hat{a}(t)\rangle$ represents the quantum fluctuation of the cavity field, and from Eq. (S5), it is found to be

$$\hat{\mathcal{A}}(t) = \exp[-i(\sigma\chi - i\kappa/2)t]\hat{\mathcal{A}}(0) - \sqrt{\kappa}\int_0^t \exp[-i(\sigma\chi - i\kappa/2)(t-s)]\hat{\mathcal{A}}_{\rm in}(s)ds. \tag{S13}$$

Since, as assumed above, the cavity subject to IES is already in a steady state at $t = 0$, we therefore have:

$$\langle\hat{\mathcal{A}}^\dagger(0)\hat{\mathcal{A}}(0)\rangle = \sinh^2(r), \qquad \langle\hat{\mathcal{A}}(0)\hat{\mathcal{A}}^\dagger(0)\rangle = 1 + \langle\hat{\mathcal{A}}^\dagger(0)\hat{\mathcal{A}}(0)\rangle, \tag{S14}$$

$$\langle\hat{\mathcal{A}}(0)\hat{\mathcal{A}}(0)\rangle = \frac{1}{2}e^{i\varphi}\sinh(2r), \quad \langle\hat{\mathcal{A}}^\dagger(0)\hat{\mathcal{A}}^\dagger(0)\rangle = \langle\hat{\mathcal{A}}(0)\hat{\mathcal{A}}(0)\rangle^*. \tag{S15}$$

With these initial conditions, we find that the measurement noise, expressed as

$$\langle \hat{M}_N^2 \rangle = \kappa \int_0^\tau \int_0^\tau dt_1 dt_2 \Big\{ \langle \hat{\mathcal{A}}_{\rm out}(t_1)\hat{\mathcal{A}}_{\rm out}(t_2)\rangle e^{-i2\phi_h} + \langle \hat{\mathcal{A}}^\dagger_{\rm out}(t_1)\hat{\mathcal{A}}_{\rm out}(t_2)\rangle + \langle \hat{\mathcal{A}}_{\rm out}(t_1)\hat{\mathcal{A}}^\dagger_{\rm out}(t_2)\rangle + \langle \hat{\mathcal{A}}^\dagger_{\rm out}(t_1)\hat{\mathcal{A}}^\dagger_{\rm out}(t_2)\rangle e^{i2\phi_h} \Big\}, \tag{S16}$$

is given by

$$\begin{aligned}\langle \hat{M}_N^2 \rangle = \kappa\tau\cosh(2r) + \frac{1}{2}\Big[& 3\cos(\varphi - 2\phi_h) - (3 - 2\kappa\tau)\cos(4\sigma\psi - \varphi + 2\phi_h) \\ & + 6\sin(2\sigma\psi)\sin(4\sigma\psi - \varphi + 2\phi_h) - 16e^{-\kappa\tau/2}\cos(\sigma\psi)\sin(2\sigma\psi)\sin(3\sigma\psi - \varphi + 2\phi_h + \chi\tau) \\ & + 4e^{-\kappa\tau}\cos(\sigma\psi)\sin(2\sigma\psi)\sin(3\sigma\psi - \varphi + 2\phi_h + 2\chi\tau)\Big]\sinh(2r),\end{aligned} \tag{S17}$$

and therefore we obtain

$$\langle M_N^2 \rangle_\downarrow + \langle M_N^2 \rangle_\uparrow = 2\kappa\tau\left[\cosh(2r) + \cos(\varphi - 2\phi_h)\sinh(2r)\mathcal{F}(\tau)\right]. \tag{S18}$$

Here,

$$\begin{aligned}\mathcal{F}(\tau) = \frac{1}{2\kappa\tau}\Big\{ & 3 + 3\cos(2\psi) - (3 - 2\kappa\tau)\cos(4\psi) - 3\cos(6\psi) \\ & + 4\cos(\psi)\sin(2\psi)\left[e^{-\kappa\tau}\sin(3\psi + 2\chi\tau) - 4e^{-\kappa\tau/2}\sin(3\psi + \chi\tau)\right]\Big\}.\end{aligned} \tag{S19}$$

It is seen that for a given measurement time $\kappa\tau$, the noise, $\langle M_N^2 \rangle_\downarrow + \langle M_N^2 \rangle_\uparrow$, can be optimized for $\varphi - 2\phi_h = \pi$ if $\mathcal{F}(\tau) > 0$, or $\varphi - 2\phi_h = 0$ if $\mathcal{F}(\tau) < 0$.

In Fig. S1(a), we compare the optimal SNR of DQR using IES to that of the standard case of no squeezing; and the corresponding optimal angle ψ and squeezing parameter r are plotted in Figs. S1(b) and S1(c), respectively. It is seen from Fig. S1(a) that there is almost no improvement in the SNR at a measurement time $\tau \sim 1/\kappa$, which is the most interesting experimentally. Note that in the limits of $\kappa\tau \to 0$ and $\kappa\tau \to \infty$, we can have

$$\langle M_N^2 \rangle_\downarrow + \langle M_N^2 \rangle_\uparrow \simeq 2\kappa\tau\exp(-2r), \tag{S20}$$

which indicates an exponential decrease in the measurement noise, and in turn an exponential increase in the SNR. However, both of these limits are impractical in experiments. In the limit $\kappa\tau \to 0$, the resulting SNR is extremely small, although exponentially increased. As can be seen in Fig. S1(a), in order to have a significant increase of the

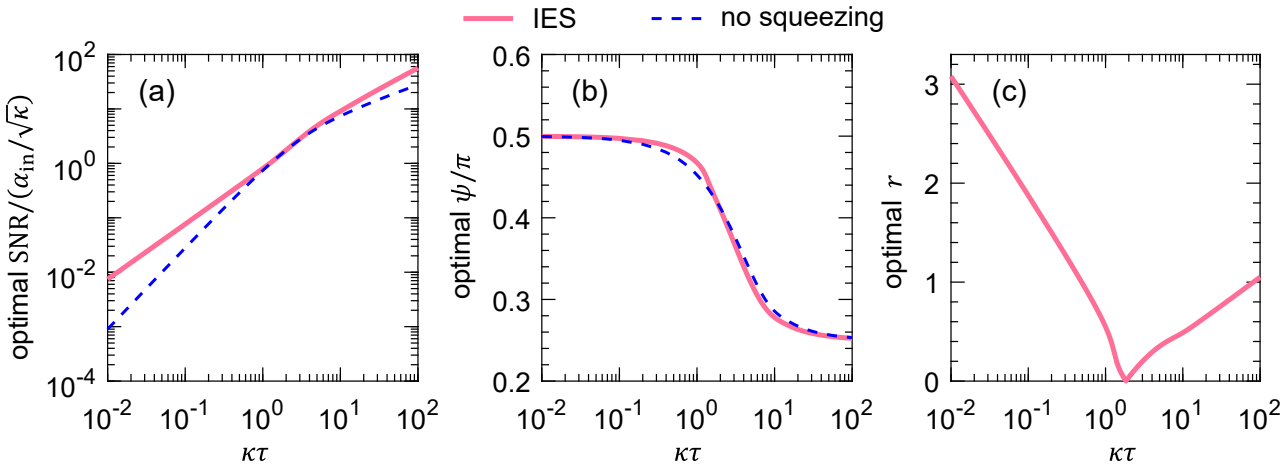

FIG. S1. Comparison of DQR with IES (solid curve) and no squeezing (dashed curve). (a) Optimal SNR as a function of the measurement time $\kappa\tau$. (b), (c) Optimal angle ψ and squeezing parameter r, corresponding to the optimal SNR in (a).

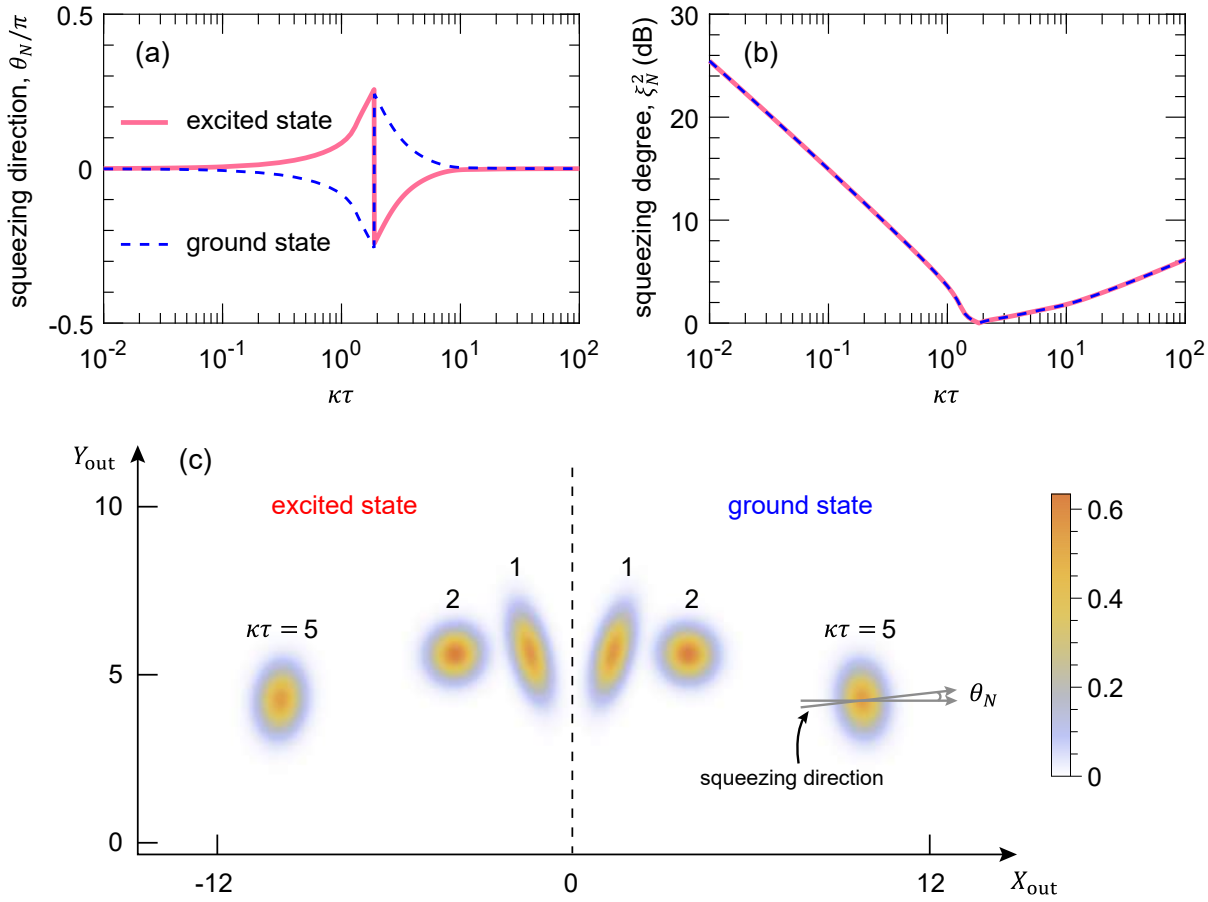

FIG. S2. (a) Squeezing direction, (b) squeezing degree, and (c) phase-space representation of the measurement noise $\langle \hat{M}_N^2 \rangle$, corresponding to the optimal SNR in Fig. S1. Solid (dashed) curves in (a) and (b), and the Wigner functions on the left- (right-) hand side of the vertical dashed line in (c) correspond to the excited (ground) state of the qubit. In (c), we chose three different measurement times, i.e., $\kappa\tau = 1$, 2, 5, as an example; $\theta_N \in [-\pi/2, \pi/2]$ refers to the angle between the squeezing direction and the horizontal axis (i.e., the measurement direction).

SNR, the measurement time τ needs to be $\sim 10^{-2}/\kappa$, at which the amplitude of the measurement tone, $\alpha_{\rm in}$, needs to be $\sim 10^2\sqrt{\kappa}$ to make the SNR larger than 1. Such a measurement tone is too strong, and is often not feasible in practice; because it can easily break down the dispersive approximation and, thus, destroy the measurement system. At the same time, as shown in Fig. S1(b), the qubit-cavity dispersive coupling χ reaches $\sim 10^2\kappa$, which is also rather unfortunate due to the fact that how to achieve such a strong nonlinearity in experiments is still an extremely challenging task. In the opposite limit $\kappa\tau \to \infty$, a significant increase in the SNR needs a measurement time much larger than $10^2/\kappa$, which, clearly, is not desired in experiments. Hence, using IES alone cannot improve the SNR in a practical manner.

In order to further understand why IES is practically not useful for DQR. In Fig. S2, we plot the squeezing direction, the squeezing degree, and the phase-space representation of the measurement noise $\langle \hat{M}_N^2 \rangle$ for the ground and excited states of the qubit for the optimal case of Fig. S1. Here, the squeezing direction is described by an angle θ_N from the horizontal axis, i.e., the measurement direction [see Fig. S2(c)], and the squeezing degree is defined as

$$\xi_N^2 = \frac{\langle \hat{M}_N^2 \rangle}{\kappa\tau}. \tag{S21}$$

Moreover, following Refs. [S1, S2], the Wigner function in phase space is defined as:

$$W\left(X_{\rm out}, Y_{\rm out}\right) = \frac{1}{2\pi\sqrt{\mathrm{Det}\left(\mathbf{D}\right)}} \exp\left(-\frac{1}{2}\mathbf{G}^{\rm T}\mathbf{D}^{-1}\mathbf{G}\right), \tag{S22}$$

where

$$\mathbf{G} = \left(X_{\rm out} - \langle \hat{X}_{\rm out}\rangle, Y_{\rm out} - \langle \hat{Y}_{\rm out}\rangle\right)^{\rm T}, \tag{S23}$$

$$\mathbf{D} = \begin{pmatrix} \langle \hat{X}_{\rm out}^2\rangle - \langle \hat{X}_{\rm out}\rangle^2 & \langle \hat{X}_{\rm out}\hat{Y}_{\rm out} + \hat{Y}_{\rm out}\hat{X}_{\rm out}\rangle/2 - \langle \hat{X}_{\rm out}\rangle\langle \hat{Y}_{\rm out}\rangle \\ \langle \hat{X}_{\rm out}\hat{Y}_{\rm out} + \hat{Y}_{\rm out}\hat{X}_{\rm out}\rangle/2 - \langle \hat{X}_{\rm out}\rangle\langle \hat{Y}_{\rm out}\rangle & \langle \hat{Y}_{\rm out}^2\rangle - \langle \hat{Y}_{\rm out}\rangle^2 \end{pmatrix}. \tag{S24}$$

Here,

$$\hat{X}_{\rm out} = \frac{1}{2}\left(\hat{A} + \hat{A}^\dagger\right), \quad \hat{Y}_{\rm out} = \frac{1}{2i}\left(\hat{A} - \hat{A}^\dagger\right), \quad \text{and} \quad \hat{A} = \frac{1}{\sqrt{\tau}}\int_0^\tau dt\, \hat{a}_{s,\rm out}(t). \tag{S25}$$

It can be readily verified that $\left[\hat{A}, \hat{A}^\dagger\right] = 1$ and $\left[\hat{X}_{\rm out}, \hat{Y}_{\rm out}\right] = i$.

Clearly, there is a direct correspondence between the results of Fig. S1 and Fig. S2. It is seen from Fig. S2(a) that with increasing the measurement time, the squeezing directions of the measurement noises $\langle \hat{M}_N^2\rangle_\downarrow$ and $\langle \hat{M}_N^2\rangle_\uparrow$ are rotated in opposite directions. In the two opposite limits $\kappa\tau \to 0$ and $\kappa\tau \to \infty$, these two squeezing directions are almost the same, thus giving an exponential but impractical increase in the SNR. However, in the experimentally most interesting regime where $\tau \sim 1/\kappa$, there is a large angle between them, as can be seen more clearly in Fig. S2(c). The presence of such an angle increases the overlap between the two pointer states. In order to reduce this overlap and achieve an optimal SNR, the squeezing degrees of the measurement noises $\langle \hat{M}_N^2\rangle_\downarrow$ and $\langle \hat{M}_N^2\rangle_\uparrow$ have to decrease (even to zero, corresponding to the perpendicular squeezing directions), as plotted in Fig. S2(b). These competing processes lead to almost no improvement of the SNR.

S2. Dispersive qubit readout with intracavity squeezing

Having discussed the case using IES, we consider in this section DQR with intracavity squeezing (ICS) generated by a two-photon driving. We demonstrate that in the case of using ICS, there also exists a rotation of squeezing similar to the case of using IES; and even worse, the degree of squeezing needs to increase gradually from the zero initial value by increasing the measurement time $\kappa\tau$. *Consequently, ICS leads to almost no improvement in the SNR at any measurement time.*

The Hamiltonian for DQR with a two-photon driven cavity reads

$$\hat{H} = \Omega\left[\hat{a}^2\exp(-i\theta) + \text{H.c.}\right] + \chi\hat{a}^\dagger\hat{a}\hat{\sigma}_z, \tag{S26}$$

where Ω and θ are the amplitude and phase of the two-photon driving, respectively. The Langevin equation of motion for the cavity mode $\hat{a}$ is accordingly given by

$$\dot{\hat{a}}(t) = -i\left(\sigma\chi - i\kappa/2\right)\hat{a} - i2\Omega\exp(i\theta)\,\hat{a}^\dagger - \sqrt{\kappa}\hat{a}_{\rm in}(t). \tag{S27}$$

Moreover, the correlations for the noise operator $\hat{\mathcal{A}}_{\rm in}(t) = \hat{a}_{\rm in}(t) - \langle\hat{a}_{\rm in}(t)\rangle$ are:

$$\langle\hat{\mathcal{A}}_{\rm in}(t)\,\hat{\mathcal{A}}_{\rm in}^\dagger(t')\rangle = [\hat{\mathcal{A}}_{\rm in}(t), \hat{\mathcal{A}}_{\rm in}^\dagger(t')] = \delta(t-t'), \tag{S28}$$

$$\langle\hat{\mathcal{A}}_{\rm in}^\dagger(t)\,\hat{\mathcal{A}}_{\rm in}(t')\rangle = \langle\hat{\mathcal{A}}_{\rm in}(t)\,\hat{\mathcal{A}}_{\rm in}(t')\rangle = 0. \tag{S29}$$

According to Eq. (S27), the cavity mode $\hat{a}$ is found to be

$$\begin{aligned}\hat{a}(t) = {}& \Lambda(t)a(0) - \Gamma(t)a^\dagger(0) \\ & - \sqrt{\kappa}\int_0^t ds\Lambda(t-s)a_{\rm in}(s) + \sqrt{\kappa}\int_0^t ds\Gamma(t-s)a_{\rm in}^\dagger(s),\end{aligned} \tag{S30}$$

where

$$\Lambda(t) = \frac{1}{\lambda}\left[\lambda\cos(\lambda t) - i\sigma\chi\sin(\lambda t)\right]\exp(-\kappa t/2), \tag{S31}$$

$$\Gamma(t) = \frac{2}{\lambda}ie^{i\theta}\Omega\sin(\lambda t)\exp(-\kappa t/2), \tag{S32}$$

$$\lambda = \sqrt{\chi^2 - 4\Omega^2}. \tag{S33}$$

As a direct result of Eq. (S30), the averaged cavity field is given, under the initial condition of $\langle \hat{a}\,(0)\rangle = 0$, by

$$\begin{aligned}\langle \hat{a}\,(t)\rangle = \frac{2\sqrt{\kappa}\alpha_{\rm in}}{\kappa^2+4\lambda^2}\Big\{ & i4\Omega e^{i(\theta-\phi_{\rm in})} - (\kappa - i2\sigma\chi)e^{i\phi_{\rm in}} \\ & - \frac{1}{\lambda}\left[(2\lambda^2 + i\kappa\sigma\chi)e^{i\phi_{\rm in}} + i2\Omega\kappa e^{i(\theta-\phi_{\rm in})}\right]\sin(\lambda t)e^{-\kappa t/2} \\ & + \left[(\kappa - i2\sigma\chi)e^{i\phi_{\rm in}} - i4\Omega e^{i(\theta-\phi_{\rm in})}\right]\cos(\lambda t)e^{-\kappa t/2}\Big\}. \end{aligned} \tag{S34}$$

It is seen that in order to stabilize the system, we need to restrict our discussions to the case either when λ is a real number (i.e., $\chi > 2\Omega$) or an imaginary number but with $|\lambda| < \kappa/2$. It then follows, according to the input-output relation $\hat{a}_{\rm out}\,(t) = \hat{a}_{\rm in}\,(t) + \sqrt{\kappa}\hat{a}\,(t)$, that

$$\langle \hat{M}\rangle_{\uparrow} - \langle \hat{M}\rangle_{\downarrow} = \frac{16(\chi/\kappa)\alpha_{\rm in}}{\sqrt{\kappa}}\cos^2(\psi)\sin(\phi_h - \phi_{\rm in})\left\{\kappa\tau - 4\cos^2(\psi)\left[1 - \frac{\sin(2\psi+\lambda\tau)}{\sin(2\psi)}e^{-\kappa\tau/2}\right]\right\}. \tag{S35}$$

Note that here, we have defined $\tan(\psi) = 2\lambda/\kappa$, instead of $\tan(\psi) = 2\chi/\kappa$ as in Sec. S1.

Furthermore, the quantum fluctuation operator of the cavity field $\hat{a}(t)$ is given by

$$\hat{\mathcal{A}}(t) = \Lambda(t)\hat{\mathcal{A}}(0) - \Gamma(t)\hat{\mathcal{A}}^{\dagger}(0) - \sqrt{\kappa}\int_0^t ds\Lambda(t-s)\hat{\mathcal{A}}_{\rm in}(s) + \sqrt{\kappa}\int_0^t ds\Gamma(t-s)\hat{\mathcal{A}}^{\dagger}_{\rm in}(s), \tag{S36}$$

according to Eq. (S30). We further assume that the two-photon driven cavity is already in a steady state at the initial measurement time $t = 0$. Under this assumption, the correlations for the cavity-field noise operator $\hat{\mathcal{A}}(0)$ read:

$$\langle \hat{\mathcal{A}}^{\dagger}(0)\hat{\mathcal{A}}(0)\rangle = \frac{8\Omega^2}{\kappa^2 - 16\Omega^2}, \qquad \langle \hat{\mathcal{A}}(0)\hat{\mathcal{A}}^{\dagger}(0)\rangle = 1 + \langle \hat{\mathcal{A}}^{\dagger}(0)\hat{\mathcal{A}}(0)\rangle, \tag{S37}$$

$$\langle \hat{\mathcal{A}}(0)\hat{\mathcal{A}}(0)\rangle = -ie^{i\theta}\frac{2\kappa\Omega}{\kappa^2 - 16\Omega^2}, \quad \langle \hat{\mathcal{A}}^{\dagger}(0)\hat{\mathcal{A}}^{\dagger}(0)\rangle = \langle \hat{\mathcal{A}}(0)\hat{\mathcal{A}}(0)\rangle^{*}. \tag{S38}$$

Then after a straightforward but tedious calculation, we find the measurement noise to be

$$\langle \hat{M}_N^2\rangle = \mathcal{G}_0(\tau) - \sin(2\phi_h - \theta)\mathcal{G}_s(\tau) + \frac{\sigma\chi}{\kappa}\cos(2\phi_h - \theta)\mathcal{G}_c(\tau), \tag{S39}$$

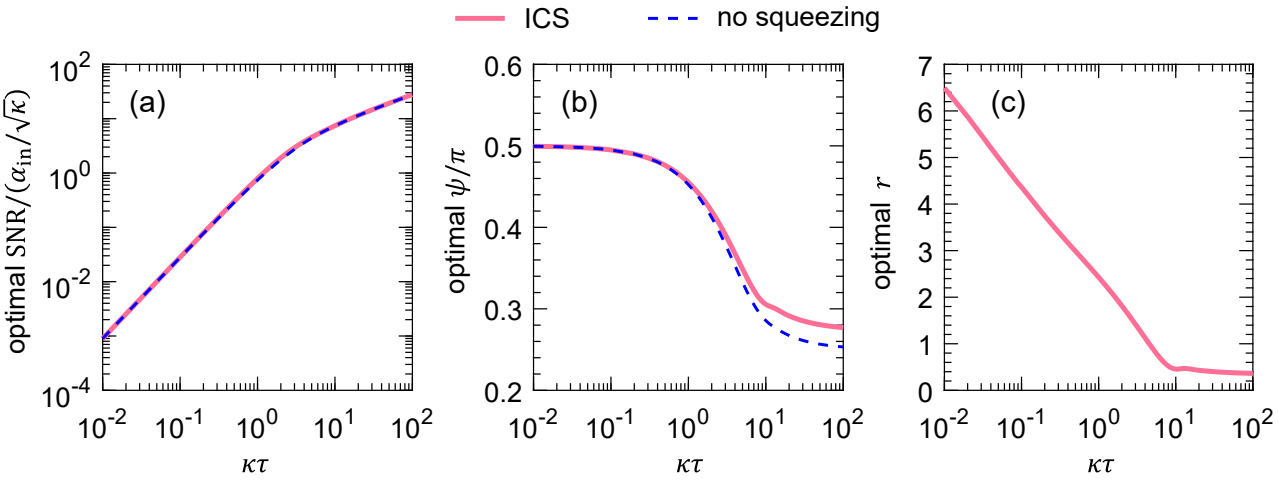

FIG. S3. Comparison of DQR with ICS (solid curve) and no squeezing (dashed curve). (a) Optimal SNR as a function of the measurement time $\kappa\tau$. (b), (c) Optimal angle ψ and squeezing parameter r, corresponding to the optimal SNR in (a). In (b), $\tan(\psi) = 2\lambda/\kappa$ for the readout with ICS, but $\tan(\psi) = 2\chi/\kappa$ for the standard case of no squeezing.

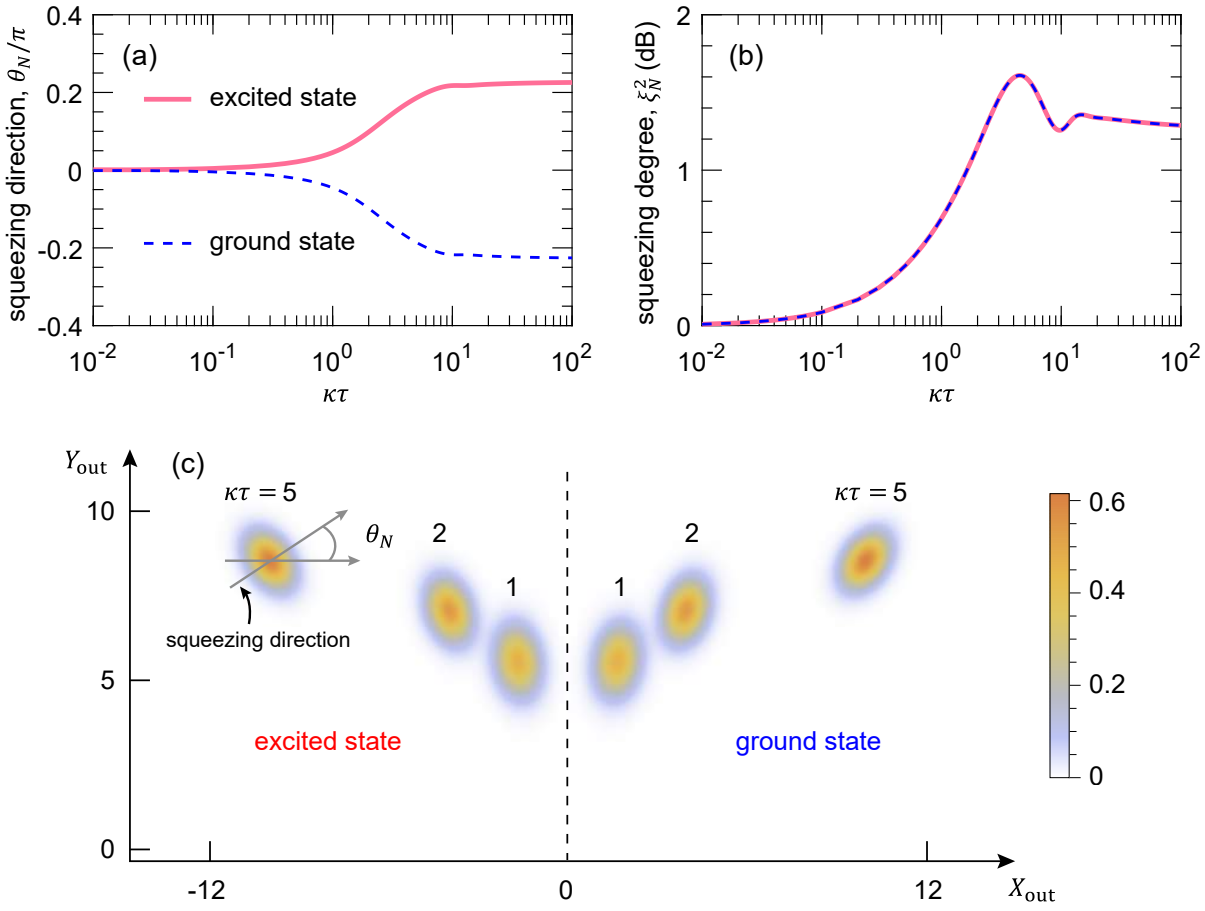

FIG. S4. (a) Squeezing direction, (b) squeezing degree, and (c) phase-space representation of the measurement noise $\langle \hat{M}_N^2 \rangle$, corresponding to the optimal SNR in Fig. S3. Solid (dashed) curves in (a) and (b), and the Wigner functions on the left- (right-) hand side of the vertical dashed line in (c) correspond to the excited (ground) state of the qubit. In (c), we chose three different measurement times, i.e., $\kappa\tau = 1$, 2, 5, as an example; $\theta_N \in [-\pi/2, \pi/2]$ refers to the angle between the squeezing direction and the horizontal axis (i.e., the measurement direction).

where

$$\begin{aligned}\mathcal{G}_0(\tau) = \frac{1}{2}\kappa\tau \Big\{ & 1 + \cosh(r) + [5 + 8\cos(2\psi) + 2\cos(4\psi) - \cosh(r)]\tanh^2(\frac{r}{2}) \Big\} \\ & - 2\cos^2(\psi)\{5 + 3\cos(4\psi) + \cos(2\psi)[9 - 2\cosh(r)] - 3\cosh(r)\}\tanh^2(\frac{r}{2}) \\ & - e^{-\kappa\tau}[2 - \cos(2\psi + 2\lambda\tau) - \cos(4\psi + 2\lambda\tau)][\cos(2\psi) - \cosh(r)]\cot^2(\psi)\tanh^2(\frac{r}{2}) \\ & - 8e^{-\kappa\tau/2}\cos^2(\psi)\tanh^2(\frac{r}{2})\Big\{ [\cos(\lambda\tau) - \cot(\psi)\sin(4\psi + \lambda\tau)]\cosh^2(\frac{r}{2}) \\ & + 4\cos^2(\psi)\cot(\psi)\sin(2\psi + \lambda\tau)\sinh^2(\frac{r}{2})\Big\},\end{aligned} \tag{S40}$$

$$\begin{aligned}\mathcal{G}_s(\tau) = & \, 2\cos^2(\psi)\{-1 - 3\cos(4\psi) + \cosh(r) + \cos(2\psi)[-3 + 2\kappa\tau + 2\cosh(r)]\}\tanh(\frac{r}{2}) \\ & - 2e^{-\kappa\tau}\cos(\psi)\cot(\psi)\sin(3\psi + 2\lambda\tau)[\cos(2\psi) - \cosh(r)]\tanh(\frac{r}{2}) \\ & - 4e^{-\kappa\tau/2}\cos(\psi)\cot(\psi)\left[\sin(3\psi + \lambda\tau)\sinh(r) - 2\cos(\psi)\sin(4\psi + \lambda\tau)\tanh(\frac{r}{2})\right],\end{aligned} \tag{S41}$$

$$\begin{aligned}\mathcal{G}_c(\tau) = {} & 8\cos^4(\psi)\left[3-2\kappa\tau+6\cos(2\psi)-2\cosh(r)\right]\tanh(\frac{r}{2}) \\ & -16e^{-\kappa\tau/2}\cos^4(\psi)\cot(\psi)\sinh^2(\frac{r}{2})\left[\coth(\frac{r}{2})\sec^2(\psi)\sin(4\psi+\lambda\tau)-4\sin(2\psi+\lambda\tau)\tanh(\frac{r}{2})\right] \\ & +8e^{-\kappa\tau}\cos^2(\psi)\sinh(\frac{r}{2})\Big\{\cos(\psi)\cos(3\psi+2\lambda\tau)\cosh(\frac{r}{2}) \\ & -\left[1-\cos(\psi)\cos(3\psi+2\lambda\tau)\right]\cot^2(\psi)\sinh(\frac{r}{2})\tanh(\frac{r}{2})\Big\}. \end{aligned} \tag{S42}$$

Here, we have defined a squeezing parameter,

$$r = \ln\left(\frac{\kappa+4\Omega}{\kappa-4\Omega}\right), \tag{S43}$$

which, in fact, determines the squeezing degree of the output field of the two-photon driven cavity in the absence of the qubit. Consequently, we have

$$\langle\hat{M}_N^2\rangle_\downarrow + \langle\hat{M}_N^2\rangle_\uparrow = 2\mathcal{G}_0(\tau) - 2\sin(2\phi_h-\theta)\mathcal{G}_s(\tau). \tag{S44}$$

It is seen that for a given measurement time $\kappa\tau$, the noise, $\langle\hat{M}_N^2\rangle_\downarrow + \langle\hat{M}_N^2\rangle_\uparrow$, can be optimized for $2\phi_h-\theta=\pi/2$ if $\mathcal{G}_s(\tau)>0$, or for $2\phi_h-\theta=-\pi/2$ if $\mathcal{G}_s(\tau)<0$. The number of cavity photons is accordingly given by

$$n(t) = \langle\hat{a}^\dagger(t)\,\hat{a}(t)\rangle = \frac{1}{8}\left[4\cos^2(\psi)-e^{-\kappa t}\mathcal{Q}_0\right]\tanh^2(\frac{r}{2}) + \left(\frac{\alpha_{\rm in}}{\sqrt{\kappa}}\right)^2\mathcal{Q}_1,$$

where

$$\mathcal{Q}_0 = \left[2-\cos(2\lambda t)-\cos(2\psi+2\lambda t)\right]\left[\cos(2\psi)-\cosh(r)\right]\csc^2(\psi), \tag{S45}$$

$$\begin{aligned}\mathcal{Q}_1 = {} & 4\left(\frac{\alpha_{\rm in}}{\sqrt{\kappa}}\right)^2\cos^2(\psi)\Big\{1+e^{-\kappa t}-2e^{-\kappa t/2}\cos(\lambda t) \\ & +\left[\sin(2\psi)-2e^{-\kappa t/2}\sin(2\psi+\lambda t)+e^{-\kappa t}\sin(2\psi+2\lambda t)\right]\cot(\psi)\tanh(\frac{r}{2}) \\ & +2\left[\cos(\psi)-e^{-\kappa t/2}\cot(\psi)\sin(\psi+\lambda t)\right]^2\tanh^2(\frac{r}{2})\Big\}. \end{aligned} \tag{S46}$$

In Fig. S3(a), we compare the optimal SNR of DQR using ICS (i.e., using a two-photon driven cavity) to that of the standard case of no squeezing; and the corresponding optimal angle ψ and squeezing parameter r are plotted in Figs. S3(b) and S3(c), respectively. It is seen that there is almost no improvement in the SNR for any measurement time.

We now discuss the physical reasons why the SNR can hardly be improved by ICS. In analogy to the analysis of the case of using IES in Sec. S1, we plot in Fig. S4 the squeezing direction θ_N, the squeezing degree ξ_N^2, and the phase-space representation of the measurement noise $\langle\hat{M}_N^2\rangle$ for the ground and excited states of the qubit for the optimal case of Fig. S3. We find from Figs. S4(a) and S4(b) that, when $\kappa\tau\to 0$, the squeezing directions of the measurement noises $\langle\hat{M}_N^2\rangle_\downarrow$ and $\langle\hat{M}_N^2\rangle_\uparrow$ are almost the same, but at the same time, their squeezing degrees are extremely weak. Moreover, as $\kappa\tau$ increases, the squeezing degrees are increased and gradually converged to a value of $\simeq 1.27$ dB in the limit $\kappa\tau\to\infty$; but at the same time, the squeezing directions are rotated in opposite directions as can be seen more clearly in Fig. S4(c), and they even become mutually perpendicular in the limit $\kappa\tau\to\infty$. These features prevent the SNR improvement from using ICS.

S3. Qubit-cavity dispersive coupling enhanced by squeezing

The $\hat{\sigma}_z$ term in Eq. (5) in the main article corresponds to an enhanced dispersive coupling between the qubit and the Bogoliubov mode $\hat{\beta}$, which is of the form

$$\hat{V}_{\rm sq} = \chi_{\rm sq}\hat{\beta}^\dagger\hat{\beta}\hat{\sigma}_z, \tag{S47}$$

where $\chi_{\rm sq}$ is the dispersive coupling strength given by

$$\chi_{\rm sq}=g^2\left[\frac{\cosh^2(r)}{\Delta_q-\omega_{\rm sq}}+\frac{\sinh^2(r)}{\Delta_q+\omega_{\rm sq}}\right]=\chi\left[\cosh(r)+\frac{\sinh^2(r)}{\cosh(r)+2\omega_{\rm sq}\epsilon/g}\right]. \tag{S48}$$

Here, we have defined

$$\chi=g\epsilon, \tag{S49}$$

with

$$\epsilon=\frac{g\cosh(r)}{\Delta_q-\omega_{\rm sq}}. \tag{S50}$$

Note that a very recent experiment [S3] in superconducting circuits has demonstrated this enhanced dispersive coupling and, particularly, the increase of $\chi_{\rm sq}$ with the squeezing parameter r.

In order to better understand the physical meaning of the dispersive coupling $\hat{V}_{\rm sq}$, we now present its detailed derivation. We begin with the full Hamiltonian in Eq. (1) in the main article and, for convenience, we reproduce it here,

$$\hat{H}=\Delta_c\hat{a}^\dagger\hat{a}+\frac{1}{2}\Delta_q\hat{\sigma}_z+g\left(\hat{a}^\dagger\hat{\sigma}_-+\hat{a}\hat{\sigma}_+\right)+\Omega\left(e^{i\theta}\hat{a}^{\dagger 2}+e^{-i\theta}\hat{a}^2\right). \tag{S51}$$

Upon introducing a Bogoliubov mode

$$\hat{\beta}=\cosh(r_c)\hat{a}+e^{i\theta}\sinh(r_c)\hat{a}^\dagger, \tag{S52}$$

with $\tanh(2r_c)=2\Omega/\Delta_c$, the cavity Hamiltonian is diagonalized, yielding

$$\Delta_c\hat{a}^\dagger\hat{a}+\Omega\left(e^{i\theta}\hat{a}^{\dagger 2}+e^{-i\theta}\hat{a}^2\right)=\omega_{\rm sq}\hat{\beta}^\dagger\hat{\beta}, \tag{S53}$$

where $\omega_{\rm sq}=\sqrt{\Delta_c^2-4\Omega^2}$ is the resonance frequency of the mode $\hat{\beta}$. Expressed in terms of the mode $\hat{\beta}$, the full Hamiltonian $\hat{H}$ is then transformed to

$$\hat{H}=\omega_{\rm sq}\hat{\beta}^\dagger\hat{\beta}+\frac{1}{2}\Delta_q\hat{\sigma}_z+g\cosh(r)\left(\hat{\beta}^\dagger\hat{\sigma}_-+\hat{\beta}\hat{\sigma}_+\right)-g\sinh(r)\left(e^{-i\theta}\hat{\beta}\hat{\sigma}_-+e^{i\theta}\hat{\beta}^\dagger\hat{\sigma}_+\right). \tag{S54}$$

Here, we have made a replacement $r_c\to r$, since r denotes a squeezing parameter of IES used in our proposal and, in order to improve the SNR, we need to set $r_c=r$ [see Eq. (S72) below].

Furthermore, we work within the regime

$$\epsilon\ll 1, \tag{S55}$$

so that we can make a dispersive approximation [S4], and then obtain the dispersive coupling $\hat{V}_{\rm sq}$ in Eq. (S47). Note that here, to make the dispersive approximation, we also require to satisfy the condition

$$(\Delta_q+\omega_{\rm sq})\gg g\sinh(r), \tag{S56}$$

in addition to $\epsilon\ll 1$. But since the condition in Eq. (S56) is certainly satisfied once $\epsilon\ll 1$ holds, we can therefore only consider the condition of $\epsilon\ll 1$ for the dispersive approximation.

Below, we compare the dispersive coupling $\hat{V}_{\rm sq}$ and the original dispersive coupling, with no squeezing, of the qubit and the bare cavity mode $\hat{a}$, and explain the reason why the resulting improvement in the dispersive coupling is real.

Let us first consider the original dispersive coupling in the absence of squeezing. For clarity, we begin with the Jaynes-Cummings Hamiltonian of a qubit coupled to a cavity mode, i.e.,

$$\hat{H}_0=\omega_c\hat{a}^\dagger\hat{a}+\frac{1}{2}\omega_q\hat{\sigma}_z+g\left(\hat{a}^\dagger\hat{\sigma}_-+\hat{a}\hat{\sigma}_+\right). \tag{S57}$$

In the regime where

$$\epsilon_0=\frac{g}{\omega_q-\omega_c}\ll 1, \tag{S58}$$

we can make a dispersive approximation [S4], yielding a dispersive coupling of the qubit and the cavity mode,

$$\hat{V}_0 = \chi_0 \hat{a}^\dagger \hat{a} \hat{\sigma}_z, \tag{S59}$$

where χ_0 is the dispersive coupling strength given by

$$\chi_0 = \frac{g^2}{\omega_q - \omega_c} = g\epsilon_0. \tag{S60}$$

The use of the Jaynes-Cummings interaction given in Eq. (S57) is the simplest and most common way to achieve the dispersive coupling $\hat{V}_0$.

Note that ϵ_0 is a key parameter, which determines the validity or accuracy of the dispersive approximation applied to Eq. (S57). Analogously, as described above, the parameter ϵ in Eq. (S50) determines the validity or accuracy of the dispersive approximation applied to Eq. (S54), and it plays a role similar to the parameter ϵ_0.

Thus, in order to ensure a fair comparison between the dispersive couplings $\hat{V}_0$ and $\hat{V}_{\rm sq}$, we need to assume

$$\epsilon_0 = \epsilon, \tag{S61}$$

such that the dispersive approximations applied for $\hat{V}_0$ and $\hat{V}_{\rm sq}$, respectively, can have the same validity or accuracy. In such a case, by comparing Eqs. (S49) and (S60), we see that

$$\chi_0 = \chi. \tag{S62}$$

That is, *under the condition that the two dispersive couplings $\hat{V}_0$ and $\hat{V}_{\rm sq}$ have the same validity or accuracy, the parameter χ can be regarded as the original dispersive coupling strength χ_0*. Consequently, according to Eq. (S48), our dispersive coupling strength $\chi_{\rm sq}$ can be regarded as being enhanced by a factor of

$$\cosh(r) + \frac{\sinh^2(r)}{\cosh(r) + 2\omega_{\rm sq}\epsilon/g}, \tag{S63}$$

compared to the original dispersive coupling strength χ_0 (i.e., χ). Moreover, as long as $\epsilon \ll 1$, we have

$$\cosh(r) + \frac{\sinh^2(r)}{\cosh(r) + 2\omega_{\rm sq}\epsilon/g} \simeq \exp(r) \tag{S64}$$

and as a result, an exponential enhancement,

$$\chi_{\rm sq} \simeq \chi_0 \exp(r), \quad \text{i.e.,} \quad \chi_{\rm sq} \simeq \chi \exp(r). \tag{S65}$$

Hence, according to the above discussions, our proposal leads to a real improvement in the dispersive coupling and as a result also in the SNR.

Note that in order to obtain the enhanced dispersive coupling $\hat{V}_{\rm sq}$ from Eq. (S54), we assume that the coupling strengths $g\cosh(r)$ and $g\sinh(r)$ are small, compared to the detunings $\Delta_q - \omega_{\rm sq}$ and $\Delta_q + \omega_{\rm sq}$, respectively; i.e., $\epsilon \ll 1$ [note that, as mentioned above, $\epsilon \ll 1$ ensures $(\Delta_q + \omega_{\rm sq}) \gg g\sinh(r)$]. However, in analogy, obtaining the original dispersive coupling $\hat{V}_0$ from Eq. (S57) is also based on assuming the coupling strength g to be small compared to the detuning $\omega_q - \omega_c$; i.e., $\epsilon_0 \ll 1$. To have a fair comparison, as mentioned above, we need to set $\epsilon_0 = \epsilon$. Thus, in this case, the assumption of $\epsilon \ll 1$ does not affect the improvement of the dispersive coupling.

S4. Improved dispersive qubit readout with both injected external squeezing and intracavity squeezing

In this section, we consider the case when IES and ICS are used simultaneously for DQR, and demonstrate that *for any measurement time, squeezing in this case can enable an exponential increase of the readout SNR. In particular, the short-time SNR can be increased exponentially with twice the squeezing parameter*. This is in stark contrast to the case of using IES or ICS alone.

To begin, we consider the Langevin equation of motion,

$$\dot{\hat{\beta}}(t) = -i(\omega_\sigma - i\frac{\kappa}{2})\hat{\beta} - \sqrt{\kappa}\hat{\beta}_{\rm in}(t), \tag{S66}$$

where $\omega_\sigma = \omega_{\rm sq} + \sigma\chi_{\rm sq}$, and $\hat{\beta}_{\rm in}(t)$ denotes the input field of the Bogoliubov mode $\hat{\beta}$. It is seen that the information about the qubit state is mapped onto the mode $\hat{\beta}$, rather than the bare mode $\hat{a}$. The quantum fluctuation operator, $\hat{\mathcal{B}}_{\rm in}(t) = \hat{\beta}_{\rm in}(t) - \langle\hat{\beta}_{\rm in}(t)\rangle$, of the input field $\hat{\beta}_{\rm in}(t)$, is given by

$$\hat{\mathcal{B}}_{\rm in}(t) = \cosh(r_c)\hat{\mathcal{A}}_{\rm in}(t) + e^{i\theta}\sinh(r_c)\hat{\mathcal{A}}^\dagger_{\rm in}(t), \tag{S67}$$

according to the Bogoliubov transformation,

$$\hat{\beta}_{\rm in}(t) = \cosh(r_c)\hat{a}_{\rm in}(t) + e^{i\theta}\sinh(r_c)\hat{a}^\dagger_{\rm in}(t). \tag{S68}$$

The correlations for $\hat{\mathcal{A}}_{\rm in}(t)$ are given in Eqs. (S3) and (S4) and thus, the correlations for the operator $\hat{\mathcal{B}}_{\rm in}(t)$ are found to be:

$$\langle\mathcal{B}^\dagger_{\rm in}(t)\mathcal{B}_{\rm in}(t')\rangle = \mathcal{N}\delta(t-t'), \qquad \langle\mathcal{B}_{\rm in}(t)\mathcal{B}^\dagger_{\rm in}(t')\rangle = (\mathcal{N}+1)\,\delta(t-t'), \tag{S69}$$

$$\langle\mathcal{B}_{\rm in}(t)\mathcal{B}_{\rm in}(t')\rangle = \mathcal{M}\delta(t-t'), \qquad \langle\mathcal{B}^\dagger_{\rm in}(t)\mathcal{B}^\dagger_{\rm in}(t')\rangle = \mathcal{M}^*\delta(t-t'), \tag{S70}$$

where

$$\begin{aligned}\mathcal{N} =\ & \cosh^2(r_c)\sinh^2(r) + \sinh^2(r_c)\cosh^2(r) + \frac{1}{2}\cos(\theta-\varphi)\sinh(2r_c)\sinh(2r),\\ \mathcal{M} =\ & \frac{1}{2}\Big[e^{i\varphi}\cosh^2(r_c)\sinh(2r) + e^{i\theta}\sinh(2r_c)\sinh^2(r)\\ & + e^{i\theta}\sinh(2r_c)\cosh^2(r) + e^{i(2\theta-\varphi)}\sinh^2(r_c)\sinh(2r)\Big].\end{aligned} \tag{S71}$$

This indicates that the mode $\hat{\beta}$ suffers from thermal noise, characterized by $\mathcal{N}$, and two-photon correlation noise, characterized by $\mathcal{M}$. These two types of noise are undesired in our proposal, but having

$$r_c = r, \quad \text{and} \quad \theta - \varphi = \pi \tag{S72}$$

can eliminate them completely, i.e.,

$$\mathcal{N} = \mathcal{M} = 0, \tag{S73}$$

so that the mode $\hat{\beta}$ suffers only from a simple vacuum noise, i.e.,

$$\langle\mathcal{B}_{\rm in}(t)\mathcal{B}^\dagger_{\rm in}(t')\rangle = \delta(t-t'), \tag{S74}$$

$$\langle\mathcal{B}^\dagger_{\rm in}(t)\mathcal{B}_{\rm in}(t')\rangle = \langle\mathcal{B}_{\rm in}(t)\mathcal{B}_{\rm in}(t')\rangle = \langle\mathcal{B}^\dagger_{\rm in}(t)\mathcal{B}^\dagger_{\rm in}(t')\rangle = 0. \tag{S75}$$

In this case, we show below that the measurement noise of the readout can be exponentially suppressed.

As usual, we formally integrate the equation of motion in Eq. (S66) to yield

$$\hat{\beta}(t) = \hat{\beta}(0)\exp[-i(\omega_\sigma - i\kappa/2)t] - \sqrt{\kappa}\int_0^t ds\exp[-i(\omega_\sigma - i\kappa/2)(t-s)]\hat{\beta}_{\rm in}(s), \tag{S76}$$

and accordingly, the number of cavity photons in the mode $\hat{\beta}$ is found to be

$$n(t) = \langle\hat{\beta}(t)^\dagger\hat{\beta}(t)\rangle = 4|\langle\hat{\beta}_{\rm in}(t)\rangle|^2\cos^2(\psi_\sigma)\left[1 + e^{-\kappa t} - 2e^{-\kappa t/2}\cos(\omega_\sigma t)\right], \tag{S77}$$

where $\tan(\psi_\sigma) = 2\omega_\sigma/\kappa$. Then, according to the input-output relation $\hat{\beta}_{\rm out}(t) = \hat{\beta}_{\rm in}(t) + \sqrt{\kappa}\hat{\beta}(t)$, we have

$$\hat{\beta}_{\rm out}(t) = \hat{\beta}_{\rm in}(t) + \sqrt{\kappa}\hat{\beta}(0)\exp[-i(\omega_\sigma - i\kappa/2)t] - \kappa\int_0^t ds\exp[-i(\omega_\sigma - i\kappa/2)(t-s)]\hat{\beta}_{\rm in}(s), \tag{S78}$$

and thus,

$$\hat{\mathcal{B}}_{\rm out}(t) = \hat{\beta}_{\rm out}(t) - \langle\hat{\beta}_{\rm out}(t)\rangle \tag{S79}$$

$$= \hat{\mathcal{B}}_{\rm in}(t) + \sqrt{\kappa}\hat{\mathcal{B}}(0)\exp[-i(\omega_\sigma - i\kappa/2)t] - \kappa\int_0^t ds\exp[-i(\omega_\sigma - i\kappa/2)(t-s)]\hat{\mathcal{B}}_{\rm in}(s), \tag{S80}$$

with $\hat{\mathcal{B}}(t)=\hat{\beta}(t)-\langle\hat{\beta}(t)\rangle$ being the quantum fluctuation operator of the Bogoliubov mode $\hat{\beta}$. As can be verified by a straightforward calculation, the correlations for $\hat{\mathcal{B}}_{\rm out}(t)$ are:

$$\langle\hat{\mathcal{B}}_{\rm out}(t)\hat{\mathcal{B}}^{\dagger}_{\rm out}(t')\rangle=\delta(t-t'), \tag{S81}$$

$$\langle\hat{\mathcal{B}}^{\dagger}_{\rm out}(t)\hat{\mathcal{B}}_{\rm out}(t')\rangle=\langle\hat{\mathcal{B}}_{\rm out}(t)\hat{\mathcal{B}}_{\rm out}(t')\rangle=\langle\hat{\mathcal{B}}^{\dagger}_{\rm out}(t)\hat{\mathcal{B}}^{\dagger}_{\rm out}(t')\rangle=0, \tag{S82}$$

It then follows, by using the Bogoliubov transformation

$$\hat{\mathcal{A}}_{\rm out}(t)=\hat{a}_{\rm out}(t)-\langle\hat{a}_{\rm out}(t)\rangle \tag{S83}$$

$$=\cosh(r)\hat{\mathcal{B}}_{\rm out}(t)-e^{i\theta}\sinh(r)\hat{\mathcal{B}}^{\dagger}_{\rm out}(t), \tag{S84}$$

that the correlations for $\hat{\mathcal{A}}_{\rm out}(t)$ are given by

$$\langle\hat{\mathcal{A}}^{\dagger}_{\rm out}(t)\hat{\mathcal{A}}_{\rm out}(t')\rangle=\sinh^2(r)\delta(t-t'),\qquad\langle\hat{\mathcal{A}}_{\rm out}(t)\hat{\mathcal{A}}^{\dagger}_{\rm out}(t')\rangle=\cosh^2(r)\delta(t-t'), \tag{S85}$$

$$\langle\hat{\mathcal{A}}_{\rm out}(t)\hat{\mathcal{A}}_{\rm out}(t')\rangle=-\frac{1}{2}e^{i\theta}\sinh(2r)\delta(t-t'),\qquad\langle\hat{\mathcal{A}}^{\dagger}_{\rm out}(t)\hat{\mathcal{A}}^{\dagger}_{\rm out}(t')\rangle=-\frac{1}{2}e^{-i\theta}\sinh(2r)\delta(t-t'). \tag{S86}$$

Here, we have assumed that at the initial measurement time $t=0$, the cavity field, subject to a two-photon driving and a squeezed reservoir, is already in a steady state, i.e., the vacuum state of the mode $\hat{\beta}$, such that $\langle\hat{\mathcal{B}}^{\dagger}(t_0)\hat{\mathcal{B}}(t_0)\rangle=\langle\hat{\mathcal{B}}(t_0)\hat{\mathcal{B}}(t_0)\rangle=0$. From Eq. (S16), the measurement noise $\langle\hat{M}_N^2\rangle$ takes the simple form

$$\langle\hat{M}_N^2\rangle=\kappa\tau\left[\cosh(2r)-\cos(2\phi_h-\theta)\sinh(2r)\right]. \tag{S87}$$

Clearly, for $2\phi_h-\theta=0$, we obtain

$$\langle\hat{M}_N^2\rangle=\kappa\tau\exp(-2r)=\langle\hat{M}_N^2\rangle_{\rm std}\exp(-2r), \tag{S88}$$

indicating the measurement noise is exponentially suppressed at any measurement time. Here, $\langle\hat{M}_N^2\rangle_{\rm std}=\kappa\tau$ is the measurement noise of the standard readout with no squeezing. This result is in sharp contrast to the case of using IES or ICS alone as discussed above.

Having achieved an exponentially suppressed measurement noise, let us now consider the measurement signal. We find from Eq. (S68) that

$$\langle\hat{\beta}_{\rm in}(t)\rangle=\alpha_{\rm in}\exp(i\phi_{\rm in})\left\{\cosh(r)+\sinh(r)\exp[-i(2\phi_{\rm in}-\theta)]\right\}. \tag{S89}$$

Here, we have assumed that $\langle\hat{a}_{\rm in}(t)\rangle=\alpha_{\rm in}e^{i\phi_{\rm in}}$. Since the signal separation is proportional to $|\langle\hat{\beta}_{\rm in}(t)\rangle|$ (see below), we thus choose $2\phi_{\rm in}-\theta=0$, so as to ensure an exponential increase of $|\langle\hat{\beta}_{\rm in}(t)\rangle|$ with the squeezing parameter r, yielding

$$\langle\hat{\beta}_{\rm in}(t)\rangle=\alpha_{\rm in}\exp(r)\exp(i\phi_{\rm in}). \tag{S90}$$

Then, according to Eq. (S78), we obtain

$$\langle\hat{\beta}_{\rm out}(t)\rangle=\alpha_{\rm in}\exp(r)\exp(i\phi_{\rm in})\left\{1+\frac{i\kappa}{\omega_\sigma-i\kappa/2}\left\{1-\exp[-i(\omega_\sigma-i\kappa/2)t]\right\}\right\}, \tag{S91}$$

under the initial condition of $\langle\hat{\beta}(0)\rangle=0$. Subsequently, the measurement signal, defined in Eq. (S7), is found by taking the Bogoliubov transformation $\hat{a}_{\rm out}(t)=\cosh(r)\hat{\beta}_{\rm out}(t)-e^{i\theta}\sinh(r)\hat{\beta}^{\dagger}_{\rm out}(t)$:

$$\begin{aligned}\langle\hat{M}\rangle=\frac{2\alpha_{\rm in}e^r}{\sqrt{\kappa}}\Big\{&\left[2-\kappa\tau+2\cos(2\psi_\sigma)\right]\left[\cos(\vartheta_+)\cosh(r)-\cos(\vartheta_-+\theta)\sinh(r)\right]\\&-4e^{-\kappa\tau/2}\cos^2(\psi_\sigma)\left[\cos(\vartheta_++\omega_\sigma\tau)\cosh(r)-\cos(\vartheta_-+\theta+\omega_\sigma\tau)\sinh(r)\right]\Big\},\end{aligned} \tag{S92}$$

where $\vartheta_\pm=2\psi_\sigma\pm\phi_h-\phi_{\rm in}$. We now divide the signal separation, $|\langle\hat{M}\rangle_\uparrow-\langle\hat{M}\rangle_\downarrow|$, into two components, one along the measurement direction of homodyne detection (i.e., the squeezing direction), labelled $|\langle\hat{M}\rangle_\uparrow-\langle\hat{M}\rangle_\downarrow|_\parallel$; and the other along the direction perpendicular to the measurement direction of homodyne detection (i.e., the antisqueezing

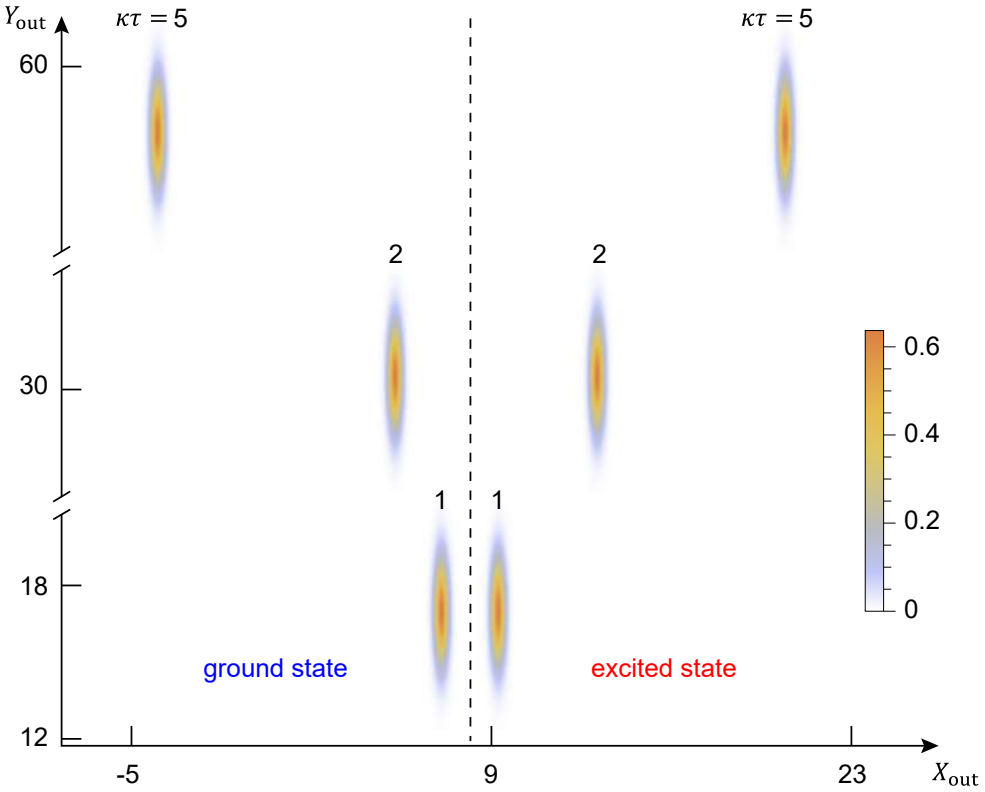

FIG. S5. Phase-space representation of DQR simultaneously using IES and ICS. The Wigner functions on the left- and right-hand sides of the vertical dashed line correspond to the ground and excited states of the qubit, respectively. Here, we assumed $\chi = 0.5\kappa$, $r = 1$ and chose three different measurement times, i.e., $\kappa\tau = 1$, 2, 5, as an example.

direction), labelled $|\langle\hat{M}\rangle_\uparrow - \langle\hat{M}\rangle_\downarrow|_\perp$. It can be seen that $|\langle\hat{M}\rangle_\uparrow - \langle\hat{M}\rangle_\downarrow|_\parallel$ and $|\langle\hat{M}\rangle_\uparrow - \langle\hat{M}\rangle_\downarrow|_\perp$ are found by setting $2\phi_h - \theta = 0$, $\phi_{\rm in} - \phi_h = 0$ and $\theta - 2\phi_h = \pi$, $\phi_{\rm in} - \phi_h = \frac{\pi}{2}$, respectively, yielding

$$
\begin{aligned}
&|\langle\hat{M}\rangle_\uparrow - \langle\hat{M}\rangle_\downarrow|_\parallel \\
&= \frac{2\alpha_{\rm in}}{\sqrt{\kappa}} \Big| \left[2 - \kappa\tau + 2\cos(2\psi_{-1}) + 2\cos(2\psi_{+1})\right] \left[\cos(2\psi_{-1}) - \cos(2\psi_{+1})\right] \\
&\quad - e^{-\kappa\tau/2} \left[\cos(\omega_{-1}\tau) + 2\cos(2\psi_{-1} + \omega_{-1}\tau) + \cos(4\psi_{-1} + \omega_{-1}\tau) - 4\cos^2(\psi_{+1})\cos(2\psi_{+1} + \omega_{+1}\tau)\right] \Big|, \qquad \text{(S93)} \\
&|\langle\hat{M}\rangle_\uparrow - \langle\hat{M}\rangle_\downarrow|_\perp \\
&= \frac{2\alpha_{\rm in} e^{2r}}{\sqrt{\kappa}} \Big| \left[2 - \kappa\tau + 2\cos(2\psi_{-1})\right] \sin(2\psi_{-1}) - \left[2 - \kappa\tau + 2\cos(2\psi_{+1})\right] \sin(2\psi_{+1}) \\
&\quad - e^{-\kappa\tau/2} \left[\sin(\omega_{-1}\tau) + 2\sin(2\psi_{-1} + \omega_{-1}\tau) + \sin(4\psi_{-1} + \omega_{-1}\tau) - 4\cos^2(\psi_{+1})\sin(2\psi_{+1} + \omega_{+1}\tau)\right] \Big|, \qquad \text{(S94)}
\end{aligned}
$$

respectively.

Intuitively, we can directly maximize $|\langle\hat{M}\rangle_\uparrow - \langle\hat{M}\rangle_\downarrow|_\parallel$ so as to maximize the SNR, but in this case, $|\langle\hat{M}\rangle_\uparrow - \langle\hat{M}\rangle_\downarrow|_\perp$, which is usually zero in the case of using IES or ICS, may be nonzero. For example, for a give measurement time $\kappa\tau = 1$ and a given dispersive coupling $\chi = 0.5\kappa$, the maximum value of $|\langle\hat{M}\rangle_\uparrow - \langle\hat{M}\rangle_\downarrow|_\parallel$ is $\simeq 0.47\alpha_{\rm in}/\sqrt{\kappa}$ with $\tan(\psi_{+1}) \simeq 6.5$ and $\tan(\psi_{-1}) \simeq 4.5$; but at the same time, the value of $|\langle\hat{M}\rangle_\uparrow - \langle\hat{M}\rangle_\downarrow|_\perp$ is found to be $\simeq 1.1\alpha_{\rm in}/\sqrt{\kappa}$. Thus for a fair comparison with the two cases of using IES and ICS separately, we require

$$
|\langle\hat{M}\rangle_\uparrow - \langle\hat{M}\rangle_\downarrow|_\perp = 0. \qquad \text{(S95)}
$$

In fact, for a given measurement time, we can exactly ensure this requirement with an appropriate effective cavity frequency $\omega_{\rm sq}$. The dependence of $\omega_{\rm sq}$ on $\kappa\tau$ is plotted in the inset in Fig. 2(a) in the main article. Furthermore,

in Fig. 2(b) in the main article, we demonstrate an exponential enhancement in the SNR under the condition in Eq. (S95). This enhancement can be understood more deeply in the phase-space representation in Fig. S5, which is in sharp contrast to the separate uses of IES and ICS shown in Figs. S2(c) and S4(c).

We consider below the SNR in the two limits of $\kappa\tau \to 0$ and ∞. In the limit of $\kappa\tau \to 0$, the effective cavity frequency $\omega_{\rm sq}$ can be found from the condition in Eq. (S95),

$$\omega_{\rm sq} \simeq \frac{2.58}{\tau}, \tag{S96}$$

which is inversely proportional to the measurement time τ [see inset in Fig. 2(a) in the main article]. As a consequence, we have

$$|\langle\hat{M}\rangle_\uparrow - \langle\hat{M}\rangle_\downarrow| = |\langle\hat{M}\rangle_\uparrow - \langle\hat{M}\rangle_\downarrow|_\parallel \simeq \frac{0.27\alpha_{\rm in}}{\sqrt{\kappa}}\tan(\psi_{\rm sq})\,(\kappa\tau)^3 \simeq 0.81\exp(r)|\langle\hat{M}\rangle_\uparrow - \langle\hat{M}\rangle_\downarrow|_{\rm std}, \tag{S97}$$

where $\tan(\psi_{\rm sq}) = 2\chi_{\rm sq}/\kappa$, such that the SNR in the limit of $\kappa\tau \to 0$ is given by

$$\mathrm{SNR} \simeq 0.81\exp(2r)\mathrm{SNR}_{\rm std}. \tag{S98}$$

Here, $|\langle\hat{M}\rangle_\uparrow - \langle\hat{M}\rangle_\downarrow|_{\rm std}$ and $\mathrm{SNR}_{\rm std}$ refer to the signal separation and the SNR, respectively, of the standard readout with no squeezing. It can be surprisingly seen from Eq. (S98) that compared to the standard readout, the SNR can be *exponentially improved with* $2r$*, rather than* r as usually expected. Such a giant improvement arises from two contributions. The first contribution comes from the exponentially suppressed measurement noise as in Eq. (S88), and the second one is due to the exponentially amplified dispersive coupling $\chi_{\rm sq}$ as in Eq. (7) in the main article and thus the exponentially amplified signal separation as in Eq. (S97).

Furthermore, in the limit of $\kappa\tau \to \infty$, the condition in Eq. (S95) gives

$$\omega_{\rm sq} \simeq \frac{\kappa}{2}\sec(\psi_{\rm sq}), \tag{S99}$$

which is independent of the measurement time [see inset in Fig. 2(a) in the main article]. This yields

$$|\langle\hat{M}\rangle_\uparrow - \langle\hat{M}\rangle_\downarrow| = |\langle\hat{M}\rangle_\uparrow - \langle\hat{M}\rangle_\downarrow|_\parallel \simeq \frac{4\alpha_{\rm in}}{\sqrt{\kappa}}\sin(\psi_{\rm sq})\kappa\tau \simeq \frac{\sin(\psi_{\rm sq})}{\sin(2\psi)}|\langle\hat{M}\rangle_\uparrow - \langle\hat{M}\rangle_\downarrow|_{\rm std}, \tag{S100}$$

and then

$$\mathrm{SNR} \simeq \frac{\sin(\psi_{\rm sq})}{\sin(2\psi)}\exp(r)\mathrm{SNR}_{\rm std}. \tag{S101}$$

Equation (S101) indicates that in the limit $\kappa\tau \to \infty$, the SNR can have an exponential improvement with the squeezing parameter r. Note that the signal separation in Eq. (S100) is not significantly changed with increasing r, compared to the standard readout. This is in contrast to the case of $\kappa\tau \to 0$. Thus, along with an exponentially suppressed measurement noise given in Eq. (S88), the SNR in the limit $\kappa\tau \to \infty$ can be improved exponentially with r, instead of $2r$, as seen in Eq. (S101). For typical parameters $e^r = 10$ and $\chi = \kappa/2$, we can obtain $\sin(\psi_{\rm sq}) \simeq \sin(2\psi)$ and, thus, $\mathrm{SNR} \simeq \exp(r)\mathrm{SNR}_{\rm std}$ in the limit $\kappa\tau \to \infty$.

Hence, according to the above discussions, we see that with increasing the measurement time from $\kappa\tau \to 0$ to $\kappa\tau \to \infty$, the improvement of the SNR is gradually changed from $\sim e^{2r}$ to $\sim e^r$, as shown in Fig. 2(b) in the main article. Furthermore, we see that the SNR improvement originates from two aspects, one of which is due to the measurement noise exponentially suppressed at any measurement time. The other aspect is due to the exponentially enhanced dispersive coupling, which can lead to an exponentially increased signal separation and thus SNR for short-time measurements, but which has almost no contribution to the improvement of the SNR for long-time measurements.

S5. Effects of parameter mismatches on the readout

Our present proposal relies on the simultaneous use of IES and ICS, and further requires to satisfy the parameter conditions in Eq. (S72). However, in realistic experiments, there are always some parameter mismatches, such that the conditions in Eq. (S72) are not satisfied perfectly. In such an imperfect case, we assume that

$$r_c = r + \delta_r, \quad \text{and} \quad \theta - \varphi = \pi + \delta_p, \tag{S102}$$

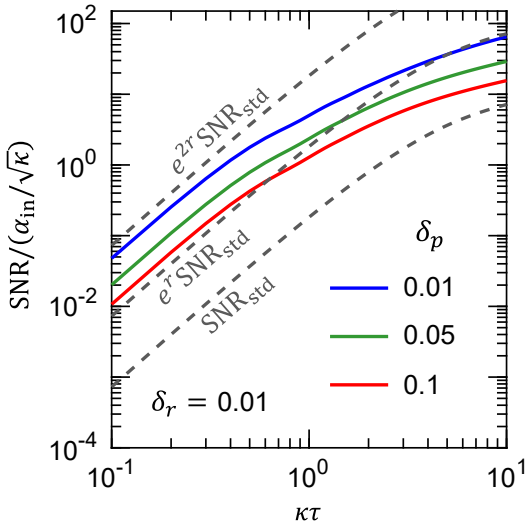

FIG. S6. SNR in the presence of parameter mismatches as a function of the measurement time $\kappa\tau$ for $\delta_p = 0.1$, 0.05, 0.01, and for $\delta_r = 0.01$. Other parameters and what the three dashed curves represent are the same as in Fig. 2(b) in the main article.

where δ_r and δ_p are the squeezing degree and direction mismatches, respectively. Below, we analyze the effects of these parameter mismatches on our readout proposal.

The ideal conditions in Eq. (S72) lead to $\mathcal{N} = \mathcal{M} = 0$, as mentioned in Sec. S4; however, due to the parameter mismatches given in Eq. (S102), $\mathcal{N}$ and $\mathcal{M}$ are no longer zero. Under such parameter mismatches, the correlations for the output noise operator $\hat{\mathcal{B}}_{\mathrm{out}}(t) = \hat{\beta}_{\mathrm{out}}(t) - \langle\hat{\beta}_{\mathrm{out}}(t)\rangle$ are found to be

$$\left\langle \hat{\mathcal{B}}_{\mathrm{out}}(t)\hat{\mathcal{B}}^{\dagger}_{\mathrm{out}}(t')\right\rangle = (\mathcal{N}+1)\,\delta(t-t') - \kappa\mathcal{N}\exp\left[-\frac{1}{2}(\kappa_\sigma t + \kappa^*_\sigma t')\right], \tag{S103}$$

$$\left\langle \hat{\mathcal{B}}_{\mathrm{out}}(t)\hat{\mathcal{B}}_{\mathrm{out}}(t')\right\rangle = \mathcal{M}\delta(t-t') - \frac{\kappa}{\kappa_\sigma}\mathcal{M}\exp\left[-\frac{1}{2}(t+t')\kappa_\sigma\right]\begin{cases}(\kappa + i2\omega_\sigma e^{\kappa_\sigma t'}) & \text{if } t \geq t',\\ (\kappa + i2\omega_\sigma e^{\kappa_\sigma t}) & \text{if } t < t',\end{cases} \tag{S104}$$

where $\kappa_\sigma = \kappa + i2\omega_\sigma$. It then follows that the measurement noise is given by

$$\left\langle \hat{M}_N^2\right\rangle = \mathcal{R}_0 + \mathcal{R}_1 + \mathcal{R}_2, \tag{S105}$$

where

$$\mathcal{R}_0 = \kappa\tau\left[\cosh(2r) + \cos(\varphi-\theta)\sinh(2r)\right], \tag{S106}$$

$$\mathcal{R}_1 = 8e^{-2r_c-\kappa\tau/2}\cos^2(\psi_\sigma)\left[\cosh(\frac{\kappa\tau}{2}) - \cos(\omega_\sigma\tau)\right]\left[1-\cosh(2r_c)\cosh(2r) - \cosh(\theta-\varphi)\sinh(2r_c)\sinh(2r)\right], \tag{S107}$$

$$\begin{aligned}\mathcal{R}_2 = e^{-2r_c-\kappa\tau}\sinh(2r_0)\cos(\psi_\sigma)\Big\{&e^{\kappa\tau}\left[(1-2\kappa\tau)\cos(\vartheta_1) - 2(1-\kappa\tau)\cos(\vartheta_3) - 3\cos(\vartheta_5)\right]\\ &+ 8e^{\kappa\tau/2}\cos(\psi_\sigma)\cos(\vartheta_4+\omega_\sigma\tau) - 4\cos^2(\psi_\sigma)\cos(\vartheta_3+2\omega_\sigma\tau)\Big\}.\end{aligned} \tag{S108}$$

Here, $\vartheta_n = n\psi_\sigma + \theta - \phi_0$. Moreover, we have set $2\phi_h - \theta = 0$, and for compact notation, defined

$$\mathcal{N} = \sinh^2(r_0), \quad \text{and} \quad \mathcal{M} = \frac{1}{2}e^{i\phi_0}\sinh(2r_0). \tag{S109}$$

Furthermore, the measurement signal $\langle\hat{M}\rangle$ is the same as in the ideal case where $\delta_p = \delta_r = 0$ [see Eq. (S92)], but with a replacement $r \to r_c$.

Having obtained the measurement noise and signal, we perform numerical simulations and plot in Fig. S6 the SNR in the presence of these parameter mismatches. It is seen that the exponential improvement in the SNR can still be

achieved even for finite parameter mismatches, suggesting that our readout proposal is experimentally feasible.

[S1] I. Strandberg, G. Johansson, and F. Quijandría, "Wigner negativity in the steady-state output of a Kerr parametric oscillator," Phys. Rev. Research **3**, 023041 (2021).

[S2] Y. Lu, I. Strandberg, F. Quijandría, G. Johansson, S. Gasparinetti, and P. Delsing, "Propagating Wigner-Negative States Generated from the Steady-State Emission of a Superconducting Qubit," Phys. Rev. Lett. **126**, 253602 (2021).

[S3] M. Villiers, W. C. Smith, A. Petrescu, A. Borgognoni, M. Delbecq, A. Sarlette, M. Mirrahimi, P. Campagne-Ibarcq, T. Kontos, and Z. Leghtas, "Dynamically Enhancing Qubit-Photon Interactions with Antisqueezing," PRX Quantum **5**, 020306 (2024).

[S4] O. Gamel and D. F. V. James, "Time-averaged quantum dynamics and the validity of the effective Hamiltonian model," Phys. Rev. A **82**, 052106 (2010).